Gate Tunable Dark Trions in Monolayer WSe$_2$

Erfu Liu,[1] Jeremiah van Baren,[1] Zhengguang Lu,[2,3] Mashael M. Altaiary,[1] Takashi Taniguchi,[4]
Kenji Watanabe,[4] Dmitry Smirnov,[2] and Chun Hung Lui[1,*]

[1]*Department of Physics and Astronomy, University of California, Riverside, California 92521, USA*
[2]*National High Magnetic Field Laboratory, Tallahassee, Florida 32310, USA*
[3]*Department of Physics, Florida State University, Tallahassee, Florida 32310, USA*
[4]*National Institute for Materials Science, Tsukuba, Ibaraki 305-004, Japan*

Monolayer WSe$_2$ is an intriguing material to explore dark exciton physics. We have measured the photoluminescence from dark excitons and trions in ultraclean monolayer WSe$_2$ devices encapsulated by boron nitride. The dark trions can be tuned continuously between negative and positive trions with electrostatic gating. We reveal their spin-triplet configuration and distinct valley optical emission by their characteristic Zeeman splitting under a magnetic field. The dark trion binding energies are 14–16 meV, slightly lower than the bright trion binding energies (21–35 meV). The dark trion lifetime ($\sim$1.3 ns) is two orders of magnitude longer than the bright trion lifetime ($\sim$10 ps) and can be tuned between 0.4 and 1.3 ns by gating. Such robust, optically detectable, and gate tunable dark trions may help us realize trion transport in two-dimensional materials.

Monolayer transition metal dichalcogenides (TMDs), such as MoS$_2$ and WSe$_2$, are remarkable two-dimensional semiconductors with strong Coulomb interactions. Their optical properties are governed by tightly bound excitons across the direct band gaps in two time-reversal valleys (K, K') [1–4]. The strong spin-orbit coupling splits both the conduction and valence bands into two subbands with opposite spins (Fig. 1) [5–8]. The spin configuration governs an exciton's optical properties. If the electron and hole come from bands with the same electron spin, their recombination can efficiently emit light. These bright excitons have a short lifetime ($<$10 ps) [9], in-plane transition dipole moment, and out-of-plane light emission (Fig. 1) [10]. However, if the electron and hole come from bands with opposite electron spins, the spin mismatch strongly suppresses their radiative recombination. They form dark excitons with long lifetime ($>$100 ps), out-of-plane transition dipole moment, and in-plane light emission (Fig. 1) [11–19].

Monolayer WSe$_2$ is an excellent material to explore dark exciton physics. Its dark exciton level lies well below the bright exciton level (Fig. 1) [7,12,20]. The dark excitons can thus accumulate a large population to achieve observable light emission [17,21–24]. We can control the charge density of the material by using electrostatic gating. In finite charge density, dark excitons can interact with the Fermi sea to form dark trions (Fig. 1) [25] (here we use "trions" to broadly refer to any correlated states between an exciton and an excitation from the Fermi sea). The dark trions are intriguing entities for research and application, but measuring them is challenging due to their low optical

activity. Recent research has revealed evidence of dark trions in monolayer WSe$_2$ under a strong in-plane magnetic field [15] and plasmonic environment [16], but there is still a lack of investigation into their detailed gate-dependent properties.

In this Letter, we measure the photoluminescence (PL) of dark trions in ultraclean monolayer WSe$_2$ devices
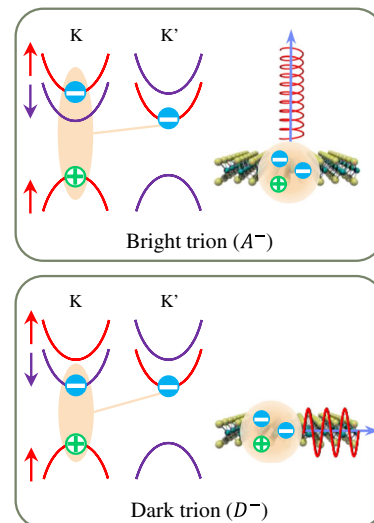

FIG. 1. Intervalley bright and dark trions in monolayer WSe$_2$. The red (blue) lines denote bands with up (down) electron spin. The shaded ellipses denote excitons involved in recombination. The bright excitons and trions emit circularly polarized light in the out-of-plane direction. The dark excitons and trions emit vertically polarized light in the in-plane direction.
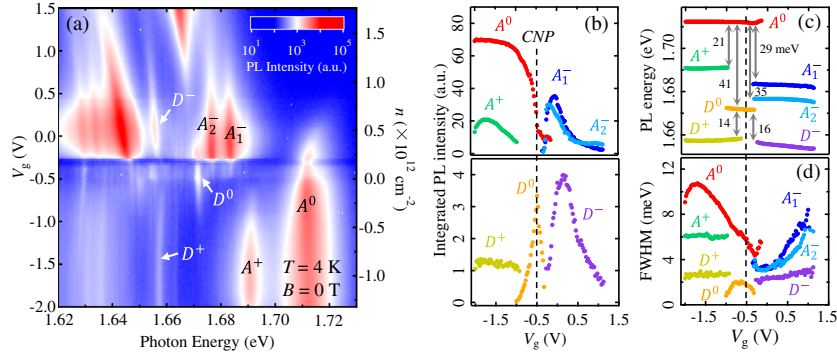
027401-1

FIG. 2. (a) Gate-dependent PL map of BN-encapsulated monolayer WSe$_2$ (device 1) at $T = 4$ K and $B = 0$ T under 532-nm continuous laser excitation. (b) The extracted PL integrated intensity, (c) PL energy, (d) PL full width at half maximum (FWHM) of both dark and bright excitons and trions as a function of gate voltage. The numbers in (c) denote the energy separation in units of meV. The dashed lines denote the charge neutrality point (CNP).

encapsulated by boron nitride (BN). The exceptional quality of our devices allows us to observe both the positive and negative dark trions under continuous electrostatic gating. Compared to bright trions with binding energies 21–35 meV, dark trions have smaller, but still sizable, binding energies (14–16 meV). We reveal the spin-triplet configuration and distinct valley optical emission of dark trions by their characteristic Zeeman splitting under a magnetic field. Their g factors (~ -9) are about twice of that of bright trions (~ -4) with spin singlet. Notably, the dark trion lifetime (1.3 ns) is two orders of magnitude longer than the bright trion lifetime (~ 10 ps). The dark trion lifetime can be tuned continuously between 0.4 and 1.3 ns by gating. Such robust, optically detectable, and gate tunable dark trions provide us with an excellent platform to explore novel excitonic physics.

We measured the PL of monolayer WSe$_2$ with 532-nm continuous laser excitation at temperature $T \sim 4$ K. We applied very low incident laser power (16 μW) to suppress the biexciton PL, which is known to be significant in monolayer WSe$_2$ [21–24]. Our samples emit weak but noticeable PL from dark excitons and trions. Although such PL propagates in the in-plane direction, we can partially capture it with a wide-angle microscope objective (NA = 0.67) in the out-of-plane detection geometry [17]. Compared to previous detection methods that require either an in-plane magnetic field, a plasmonic coupling, or a near-field tip enhancement [13–16], our detection method is much simpler and preserves the intrinsic properties of dark excitonic states.

Figure 2(a) displays a gate-dependent PL map of monolayer WSe$_2$. We observe the bright A exciton (A^0) at 1.712 meV at the charge neutrality point (gate voltage $V_g = -0.5$ V). On the electron and hole sides, one positive (A^+) and two negative (A_1^-, A_2^-) bright trions appear. Their binding energies are 21, 29, and 35 meV, respectively, consistent with prior reports [26,27]. At the charge neutrality point, a weak PL peak appears at 41 meV below the

bright exciton. This is the dark exciton (D^0) according to prior studies [14–17,21–24]. As we tune WSe$_2$ to the electron and hole sides, the D^0 peak subsides and two new peaks emerge at 16 and 14 meV below the D^0 peak. We denote them as D^- and D^+, respectively. Both the D^- and D^+ intensity increases linearly with the excitation laser power; they are thus not associated with biexcitons with quadratic power dependence [28]. We have multiple experimental evidence to support that the D^- and D^+ features come from the dark trions.

First, the D^0, D^-, and D^+ features exhibit parallel gate dependence to the bright excitons and trions. We compare the gate-dependent PL energy, intensity, and linewidth of the D^0, D^-, and D^+ peaks with those of bright excitons or trions [Figs. 2(b)–2(d)]. They exhibit parallel gate-dependent behavior. This suggests that the D^- and D^+ peaks correspond to the negative and positive dark trions, respectively. Moreover, the energy separation (14–16 meV) between the D^- and D^+ peaks and the D^0 peak matches the reported binding energy [15,28] and the theoretically predicted binding energy (~ 14 meV) [36] of dark trions in monolayer WSe$_2$.

Second, they exhibit opposite temperature dependence from the bright excitons and trions. When we decrease the temperature, the bright trion PL drops continuously, but the dark trion PL grows stronger (see Fig. S8 in the Supplemental Material [28]). Such contrasting behavior reflects their different energy levels and population distribution. The bright trions lie at a higher energy and their population drops with decreasing temperature, but the dark trions lie at the lowest energy and their population increases at low temperature (Fig. 1) [13].

Third, dark trions have a distinct spin configuration from that of bright trions. While bright trions involve a spin-singlet exciton, dark trions involve a spin-triplet exciton (see Fig. 1; the hole has the opposite spin of the valence electron) [18]. These different spin configurations can be distinguished by the Zeeman effect.
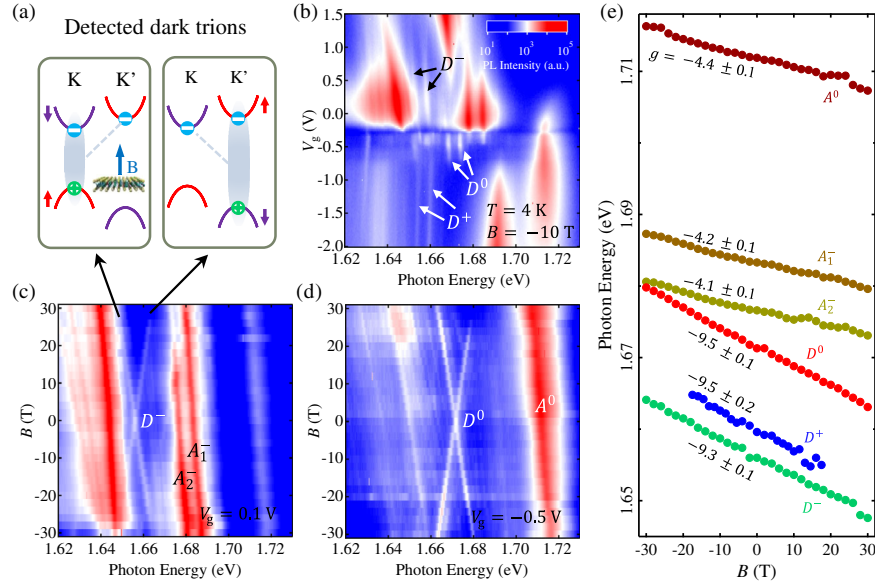
FIG. 3. (a) Negative dark trions detected in our magneto-PL experiment. (b) The PL map of monolayer WSe_2 (device 1) at $B = -10$ T under unpolarized optical excitation and right-handed PL detection. Dark excitons and trions are split into two peaks, whereas bright excitons and trions are not. (c),(d) The B-dependent PL map at the electron side ($V_g = 0.1$ V) and charge neutrality point ($V_g = -0.5$ V). (b)–(d) share the same color scale bar. (e) The excitons and trion Zeeman shifts. The g factors are extracted by linear fits of the energy difference between the positive and negative magnetic field.

Fourth, the dark trions follow different optical selection rules from those of bright trions. According to prior research, bright excitons at the K (K') valley emit light with right-handed (left-handed) circular polarization in the out-of-plane direction [6,37,38], but dark excitons at both K and K' valleys emit light with vertical linear polarization in the in-plane direction (Fig. 1) [17]. Their associated bright or dark trions follow the same optical selection rules, because the recombination of exciton is only weakly affected by its coupling to the Fermi sea [39].

We can confirm the third and fourth characteristics by PL measurements under an out-of-plane magnetic field, which lifts the valley degeneracy in monolayer TMDs [29,32,34,35]. Because of the opposite spin and orbital configurations of the K and K' valleys, the magnetic field can enlarge the band gap of one valley and diminish the band gap of the other valley [Fig. 3(a)]. The difference between the two valley gaps is defined as the valley Zeeman splitting energy $\Delta E = g\mu_B B$, where g is the effective g factor and $\mu_B = 57.88$ μeV/T is the Bohr magneton. For bright excitons and trions, their Zeeman splitting has been argued to mainly come from the orbital magnetic moment of the valance band, with an estimated g factor of about -4 [29,32,34,35]. However, for dark excitons or trions, their associated spin triplet will contribute an additional g factor of -4, making their total g factor about -8 (see Supplemental Material [28] for more discussion) [18,28,33].

To further probe the distinct optical selection rules of dark and bright trions, we adopt a special measurement

geometry—we excite monolayer WSe_2 with unpolarized light, but collect only the right-handed PL. For bright excitons or trions with circularly polarized PL, our measurement only detects the light emission from the K valley. But for dark excitons or trions with linearly polarized PL, our measurement detects emission from both valleys.

Figures 3(b)–3(d) display the gate-dependent PL map at $B = -10$ T and the B-dependent PL maps from $B = -31$ to 31 T. The spectra of bright excitons and trions remain largely unchanged except for a Zeeman shift—we detect light from only one valley, as expected. Their g factors (from -4.1 to -4.4) also match our prediction (-4) from their atomic orbits and spin-singlet configuration [Fig. 3(e)] [29,32,34,35]. In contrast, the D^0, D^-, and D^+ peaks each split into two peaks with the same energy separation—we detect light emission from both valleys, as expected from dark excitons and trions. Moreover, their g factors (from -9.3 to -9.5) roughly match our prediction (-8) from the atomic orbits and spin-triplet configuration of the dark states [Fig. 3(e)] [18,28,33]. Our experiment therefore confirms both the spin-triplet configuration and the distinct valley optical selection rules of the dark trions in monolayer WSe_2.

Dark trions are expected to live much longer than bright trions, because their spin-triplet configuration suppresses the radiative decay [15,18]. The longer lifetime of dark trions is hinted at from their narrower linewidths (FWHM $\sim$2.5 meV) compared to bright trions (FWHM = 3–9 meV) [Fig. 2(d)]. We have measured the time-resolved PL intensity of trions by the time-correlated single photon counting method
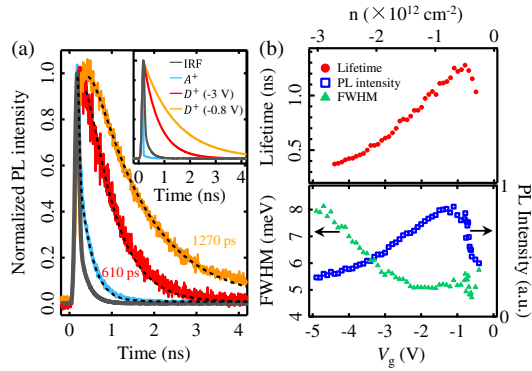
FIG. 4. (a) Time-resolved PL for the A^+ bright trion and D^+ dark trion in BN-encapsulated monolayer WSe_2 (device 2). The black solid line is the instrument response function (IRF). We fit the D^+ and A^+ data, respectively, with single-exponential and biexponential functions convolved with the IRF (dashed lines). (Inset) The deconvolved fits. The D^+ lifetime is 1270 and 610 ps at gate voltages $V_g = -0.8$ and -3 V, respectively. The A^+ lifetime is ~10 ps. (b) The lifetime, PL intensity, and FWHM of the D^+ trion as a function of gate voltage.

[Fig. 4(a)] [28]. The bright trion PL dynamics exhibits two exponential decay components. The fast and dominant component follows closely the instrument response function (IRF). We extract a lifetime of ~10 ps after deconvolution with the IRF. The slow component contributes little because it is much weaker than the fast component [inset of Fig. 4(a)] [40–42]. In contrast, the dark trion (at $V_g = -0.8$ V) shows a single exponential decay with a lifetime of 1270 ps. It is two orders of magnitude longer than the lifetime of bright excitons and trions (1–10 ps) and an order of magnitude longer than the dark exciton lifetime (180 ps) (Fig. S12) [18,28].

The lifetime of dark trions is gate tunable and correlates with the PL intensity and linewidth. Figure 4(b) displays the dark trion lifetime, PL intensity, and linewidth as a function of gate voltage (V_g). When V_g changes from 0 to −1 V in the hole side, the dark trion lifetime increases slightly from 1 to 1.3 ns, the PL intensity rises, and the linewidth remains almost constant. When V_g goes further to −4.4 V, the dark trion lifetime decreases from 1.3 to 370 ps, the PL intensity decreases, and the linewidth increases correspondingly [28]. These observations can be qualitatively understood from the interactions between trions and free carriers. When carriers are first injected into the sample, they facilitate the trion formation and enhance the trion PL. However, as their density increases, they will scatter frequently with the trions. Such scattering will shorten the trion lifetime, suppress the trion PL, and broaden the PL peak.

Prior research has shown that trions can behave like free carriers with controlled motion under an electric field [43,44]. Their charge, spin, valley, and internal energy degrees of freedom make them attractive information carriers; but, trion transport has not been achieved in atomically thin materials. One primary reason is the short lifetime of bright trions. The long-lived dark trions offer an effective solution. We may assume the trion mobility (μ) to be one-tenth of the electron-hole mobility as trions have triple the effective mass and higher scattering rate. The trion mobility can reach $\mu = 400$ cm^2 V^{-1} s^{-1} from the highest carrier mobility (4000 cm^2 V^{-1} s^{-1}) reported in monolayer WSe_2 [45]. By using an electric field $E = 0.5$ V$/\mu$m and our observed lifetime $\tau = 1$ ns, the drift distance of dark trions under an in-plane electric field can reach $l_d = \mu E \tau = 20$ μm. This distance exceeds the typical length scale of two-dimensional material devices. The long-lived, optically detectable, and gate tunable dark trions therefore provide a new path to investigate field-controlled trion transport.

Finally, we note that some researchers interpret the excitonic states under doping as exciton polarons (not trions) [46,47]. In this picture, an exciton evolves from a trion-hole state in low doping to an exciton polaron in high doping [48]. Our experimental conclusion is still valid in this picture by simply changing "dark trions" into "dark exciton polarons." The trion transport should still be realizable in the low doping regime, where the loosely bound trion-hole states easily dissociate into a trion and a free hole under an in-plane electric field.

*Corresponding author.
joshua.lui@ucr.edu

[1] K. F. Mak and J. Shan, Photonics and optoelectronics of 2D semiconductor transition metal dichalcogenides, Nat. Photonics 10, 216 (2016).

[2] X. Xu, W. Yao, D. Xiao, and T. F. Heinz, Spin and pseudospins in layered transition metal dichalcogenides, Nat. Phys. 10, 343 (2014).

[3] G. Wang, A. Chernikov, M. M. Glazov, T. F. Heinz, X. Marie, T. Amand, and B. Urbaszek, Colloquium: Excitons in atomically thin transition metal dichalcogenides, Rev. Mod. Phys. 90, 021001 (2018).

[4] H. Yu, X. Cui, X. Xu, and W. Yao, Valley excitons in two-dimensional semiconductors, Natl. Sci. Rev. 2, 57 (2015).

[5] D. Xiao, G.-B. Liu, W. Feng, X. Xu, and W. Yao, Coupled Spin and Valley Physics in Monolayers of MoS_2 and other Group-VI Dichalcogenides, Phys. Rev. Lett. 108, 196802 (2012).

[6] T. Cao, G. Wang, W. Han, H. Ye, C. Zhu, J. Shi, Q. Niu, P. Tan, E. Wang, B. Liu et al., Valley-selective circular dichroism of

monolayer molybdenum disulphide, Nat. Commun. **3**, 887 (2012).

[7] G.-B. Liu, W.-Y. Shan, Y. Yao, W. Yao, and D. Xiao, Three-band tight-binding model for monolayers of group-VIB transition metal dichalcogenides, Phys. Rev. B **88**, 085433 (2013).

[8] K. Kośmider, J. W. González, and J. Fernández-Rossier, Large spin splitting in the conduction band of transition metal dichalcogenide monolayers, Phys. Rev. B **88**, 245436 (2013).

[9] C. Robert, D. Lagarde, F. Cadiz, G. Wang, B. Lassagne, T. Amand, A. Balocchi, P. Renucci, S. Tongay, B. Urbaszek et al., Exciton radiative lifetime in transition metal dichalcogenide monolayers, Phys. Rev. B **93**, 205423 (2016).

[10] J. A. Schuller, S. Karaveli, T. Schiros, K. He, S. Yang, I. Kymissis, J. Shan, and R. Zia, Orientation of luminescent excitons in layered nanomaterials, Nat. Nanotechnol. **8**, 271 (2013).

[11] J. P. Echeverry, B. Urbaszek, T. Amand, X. Marie, and I. C. Gerber, Splitting between bright and dark excitons in transition metal dichalcogenide monolayers, Phys. Rev. B **93**, 121107(R) (2016).

[12] X.-X. Zhang, Y. You, S. Y. F. Zhao, and T. F. Heinz, Experimental Evidence for Dark Excitons in Monolayer WSe$_2$, Phys. Rev. Lett. **115**, 257403 (2015).

[13] M. R. Molas, C. Faugeras, A. O. Slobodeniuk, K. Nogajewski, M. Bartos, D. M. Basko, and M. Potemski, Brightening of dark excitons in monolayers of semiconducting transition metal dichalcogenides, 2D Mater. **4**, 021003 (2017).

[14] K.-D. Park, T. Jiang, G. Clark, X. Xu, and M. B. Raschke, Radiative control of dark excitons at room temperature by nano-optical antenna-tip Purcell effect, Nat. Nanotechnol. **13**, 59 (2018).

[15] X.-X. Zhang, T. Cao, Z. Lu, Y.-C. Lin, F. Zhang, Y. Wang, Z. Li, J. C. Hone, J. A. Robinson, D. Smirnov et al., Magnetic brightening and control of dark excitons in monolayer WSe$_2$, Nat. Nanotechnol. **12**, 883 (2017).

[16] Y. Zhou, G. Scuri, D. S. Wild, A. A. High, A. Dibos, L. A. Jauregui, C. Shu, K. De Greve, K. Pistunova, A. Y. Joe et al., Probing dark excitons in atomically thin semiconductors via near-field coupling to surface plasmon polaritons, Nat. Nanotechnol. **12**, 856 (2017).

[17] G. Wang, C. Robert, M. M. Glazov, F. Cadiz, E. Courtade, T. Amand, D. Lagarde, T. Taniguchi, K. Watanabe, B. Urbaszek et al., In-plane Propagation of Light in Transition Metal Dichalcogenide Monolayers: Optical Selection Rules, Phys. Rev. Lett. **119**, 047401 (2017).

[18] C. Robert, T. Amand, F. Cadiz, D. Lagarde, E. Courtade, M. Manca, T. Taniguchi, K. Watanabe, B. Urbaszek, and X. Marie, Fine structure and lifetime of dark excitons in transition metal dichalcogenide monolayers, Phys. Rev. B **96**, 155423 (2017).

[19] Z. Ye, T. Cao, K. O'Brien, H. Zhu, X. Yin, Y. Wang, S. G. Louie, and X. Zhang, Probing excitonic dark states in single-layer tungsten disulphide, Nature (London) **513**, 214 (2014).

[20] K. Andor, B. Guido, G. Martin, F. Jaroslav, Z. Viktor, D. D. Neil, and F. k. Vladimir, k p theory for two-dimensional transition metal dichalcogenide semiconductors, 2D Mater. **2**, 022001 (2015).

[21] M. Barbone, A. R. P. Montblanch, D. M. Kara, C. Palacios-Berraquero, A. R. Cadore, D. De Fazio, B. Pingault, E. Mostaani, H. Li, B. Chen et al., Charge-tuneable biexciton complexes in monolayer WSe$_2$, Nat. Commun. **9**, 3721 (2018).

[22] S.-Y. Chen, T. Goldstein, T. Taniguchi, K. Watanabe, and J. Yan, Coulomb-bound four- and five-particle intervalley states in an atomically-thin semiconductor, Nat. Commun. **9**, 3717 (2018).

[23] Z. Li, T. Wang, Z. Lu, C. Jin, Y. Chen, Y. Meng, Z. Lian, T. Taniguchi, K. Watanabe, S. Zhang et al., Revealing the biexciton and trion-exciton complexes in BN encapsulated WSe$_2$, Nat. Commun. **9**, 3719 (2018).

[24] Z. Ye, L. Waldecker, E. Y. Ma, D. Rhodes, A. Antony, B. Kim, X.-X. Zhang, M. Deng, Y. Jiang, Z. Lu et al., Efficient generation of neutral and charged biexcitons in encapsulated WSe$_2$ monolayers, Nat. Commun. **9**, 3718 (2018).

[25] M. Danovich, V. Zólyomi, and V. I. Fal'ko, Dark trions and biexcitons in WS$_2$ and WSe$_2$ made bright by e-e scattering, Sci. Rep. **7**, 45998 (2017).

[26] A. M. Jones, H. Yu, N. J. Ghimire, S. Wu, G. Aivazian, J. S. Ross, B. Zhao, J. Yan, D. G. Mandrus, D. Xiao et al., Optical generation of excitonic valley coherence in monolayer WSe$_2$, Nat. Nanotechnol. **8**, 634 (2013).

[27] E. Courtade, M. Semina, M. Manca, M. M. Glazov, C. Robert, F. Cadiz, G. Wang, T. Taniguchi, K. Watanabe, M. Pierre et al., Charged excitons in monolayer WSe$_2$: Experiment and theory, Phys. Rev. B **96**, 085302 (2017).

[28] See Supplemental Material at http://link.aps.org/supplemental/10.1103/PhysRevLett.123.027401 for detailed description of experimental conditions, additional data, and discussions, which includes Refs. [12,15–17, 21–24, 29–35].

[29] D. MacNeill, C. Heikes, K. F. Mak, Z. Anderson, A. Kormányos, V. Zólyomi, J. Park, and D. C. Ralph, Breaking of Valley Degeneracy by Magnetic Field in Monolayer MoSe$_2$, Phys. Rev. Lett. **114**, 037401 (2015).

[30] J. S. Ross, S. Wu, H. Yu, N. J. Ghimire, A. M. Jones, G. Aivazian, J. Yan, D. G. Mandrus, D. Xiao, W. Yao et al., Electrical control of neutral and charged excitons in a monolayer semiconductor, Nat. Commun. **4**, 1474 (2013).

[31] P. Nagler, M. V. Ballottin, A. A. Mitioglu, F. Mooshammer, N. Paradiso, C. Strunk, R. Huber, A. Chernikov, P. C. M. Christianen, C. Schüller et al., Giant magnetic splitting inducing near-unity valley polarization in van der Waals heterostructures, Nat. Commun. **8**, 1551 (2017).

[32] G. Aivazian, Z. Gong, A. M. Jones, R.-L. Chu, J. Yan, D. G. Mandrus, C. Zhang, D. Cobden, W. Yao, and X. Xu, Magnetic control of valley pseudospin in monolayer WSe$_2$, Nat. Phys. **11**, 148 (2015).

[33] M. Van der Donck, M. Zarenia, and F. M. Peeters, Strong valley Zeeman effect of dark excitons in monolayer transition metal dichalcogenides in a tilted magnetic field, Phys. Rev. B **97**, 081109(R) (2018).

[34] Y. Li, J. Ludwig, T. Low, A. Chernikov, X. Cui, G. Arefe, Y. D. Kim, A. M. van der Zande, A. Rigosi, H. M. Hill et al., Valley Splitting and Polarization by the Zeeman Effect in Monolayer MoSe$_2$, Phys. Rev. Lett. **113**, 266804 (2014).

[35] A. Srivastava, M. Sidler, A. V. Allain, D. S. Lembke, A. Kis, and A. Imamoğlu, Valley Zeeman effect in elementary optical excitations of monolayer WSe$_2$, Nat. Phys. **11**, 141 (2015).

[36] T. Deilmann and K. S. Thygesen, Dark excitations in monolayer transition metal dichalcogenides, Phys. Rev. B **96**, 201113(R) (2017).

[37] K. F. Mak, K. He, J. Shan, and T. F. Heinz, Control of valley polarization in monolayer MoS$_2$ by optical helicity, Nat. Nanotechnol. **7**, 494 (2012).

[38] H. Zeng, J. Dai, W. Yao, D. Xiao, and X. Cui, Valley polarization in MoS$_2$ monolayers by optical pumping, Nat. Nanotechnol. **7**, 490 (2012).

[39] K. F. Mak, K. He, C. Lee, G. H. Lee, J. Hone, T. F. Heinz, and J. Shan, Tightly bound trions in monolayer MoS$_2$, Nat. Mater. **12**, 207 (2013).

[40] B. Deveaud, F. Clérot, N. Roy, K. Satzke, B. Sermage, and D. S. Katzer, Enhanced Radiative Recombination of Free Excitons in GaAs Quantum Wells, Phys. Rev. Lett. **67**, 2355 (1991).

[41] T. Amand, J. Barrau, X. Marie, N. Lauret, B. Dareys, M. Brousseau, and F. Laruelle, Optical detection of vertical transport in GaAs/Al$_x$Ga$_{1-x}$As superlattices: Stationary and dynamical approaches, Phys. Rev. B **47**, 7155 (1993).

[42] G. Wang, L. Bouet, D. Lagarde, M. Vidal, A. Balocchi, T. Amand, X. Marie, and B. Urbaszek, Valley dynamics probed through charged and neutral exciton emission in monolayer WSe$_2$, Phys. Rev. B **90**, 075413 (2014).

[43] C. H. Lui, A. J. Frenzel, D. V. Pilon, Y. H. Lee, X. Ling, G. M. Akselrod, J. Kong, and N. Gedik, Trion-Induced Negative Photoconductivity in Monolayer MoS$_2$, Phys. Rev. Lett. **113**, 166801 (2014).

[44] D. Sanvitto, F. Pulizzi, A. J. Shields, P. C. M. Christianen, S. N. Holmes, M. Y. Simmons, D. A. Ritchie, J. C. Maan, and M. Pepper, Observation of charge transport by negatively charged excitons, Science **294**, 837 (2001).

[45] H. C. P. Movva, A. Rai, S. Kang, K. Kim, B. Fallahazad, T. Taniguchi, K. Watanabe, E. Tutuc, and S. K. Banerjee, High-mobility holes in dual-gated WSe$_2$ field-effect transistors, ACS Nano **9**, 10402 (2015).

[46] D. K. Efimkin and A. H. MacDonald, Many-body theory of trion absorption features in two-dimensional semiconductors, Phys. Rev. B **95**, 035417 (2017).

[47] M. Sidler, P. Back, O. Cotlet, A. Srivastava, T. Fink, M. Kroner, E. Demler, and A. Imamoglu, Fermi polaron-polaritons in charge-tunable atomically thin semiconductors, Nat. Phys. **13**, 255 (2017).

[48] Y.-C. Chang, S.-Y. Shiau, and M. Combescot, Crossover from trion-hole complex to exciton-polaron in n-doped two-dimensional semiconductor quantum wells, Phys. Rev. B **98**, 235203 (2018).